

# Study of Au-Co ultrafine grained alloy by synchrotron radiation diffractometry

T.P. Tolmachev<sup>1,2,3</sup>, V.P. Pilyugin<sup>2,3</sup>, A.M. Ancharov<sup>4,5,6</sup>, A.M. Patselov<sup>2</sup>,  
E.G. Chernyshev<sup>2</sup>, Yu.V. Solov'eva<sup>7</sup>

<sup>1</sup>The Institute of Engineering Science of UB RAS, Yekaterinburg

<sup>2</sup>M.N. Mikheev Institute of Metal Physics of UB RAS, Yekaterinburg

<sup>3</sup>Ural Federal University, Yekaterinburg

<sup>4</sup>Institute of Solid State Chemistry and Mechanochemistry, SB RAS, Novosibirsk

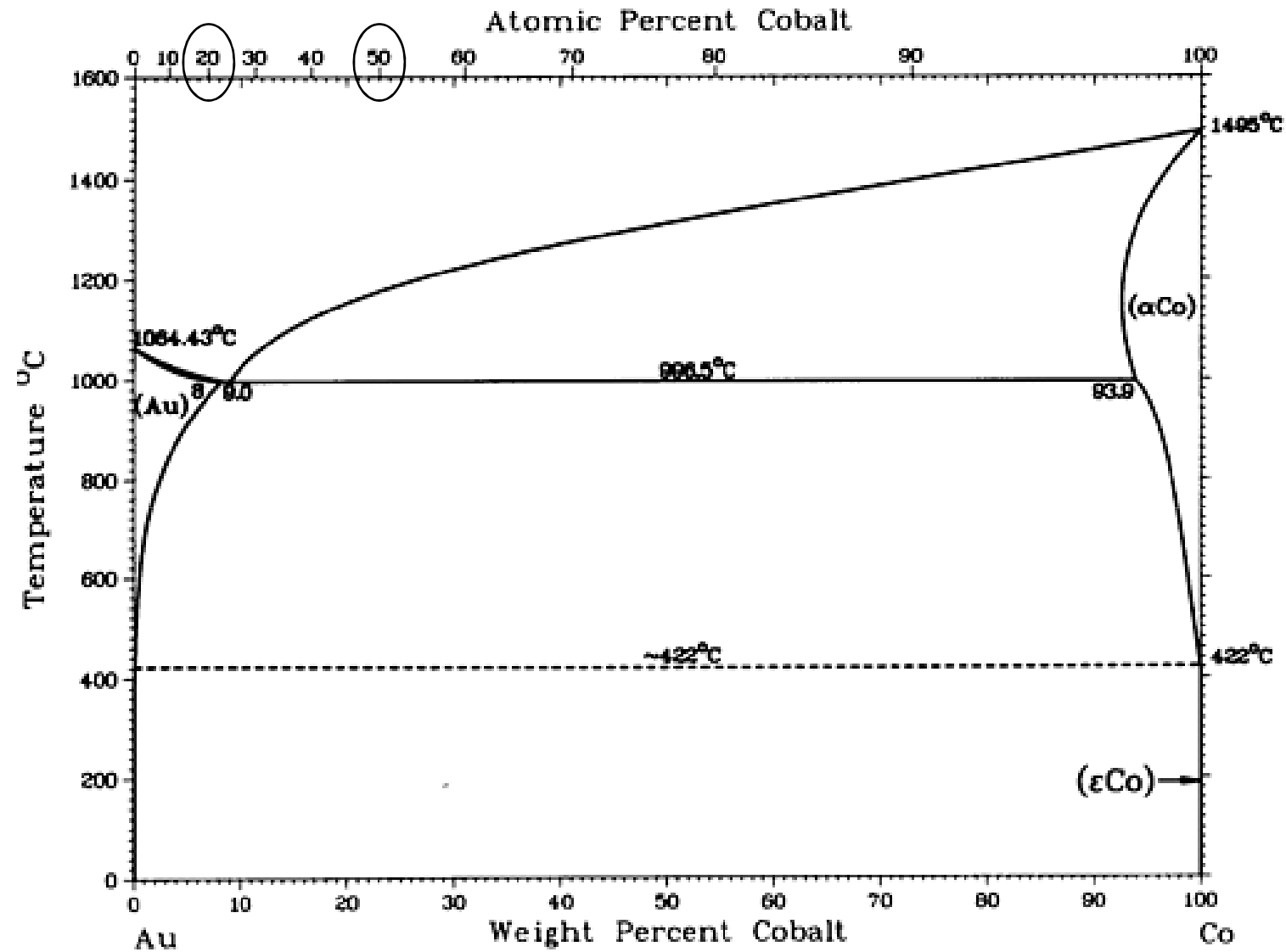
<sup>5</sup>Budker Institute of Nuclear Physics of SB RAS, Novosibirsk

<sup>6</sup>Novosibirsk State University, Novosibirsk

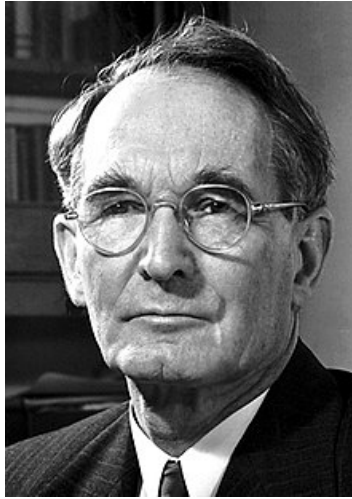
<sup>7</sup>Tomsk State University of Architecture and Building, Tomsk

# Introduction

- Au-Co alloys are of a scientific interest because of the purpose to mix Au and Co properties. Especially as a material where ferromagnetic particles embedded into a non-magnetic matrix
- Au-Co has limited solubility, high positive enthalpy of mixing (+34 kJ / mol), great difference in the characteristics of the components among themselves, there are no intermetallics on the equilibrium phase diagram



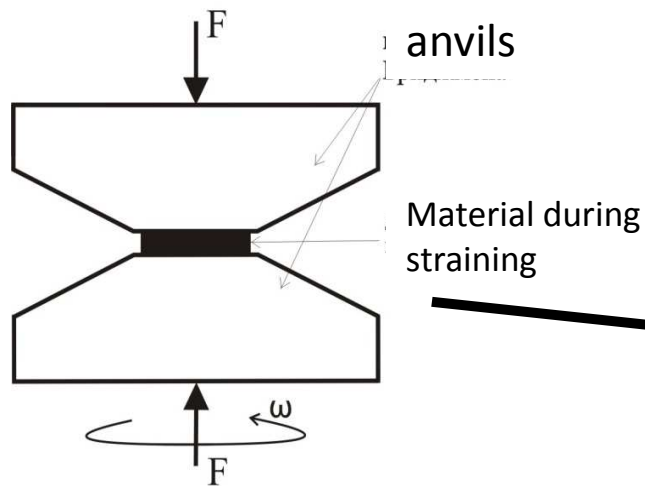
ASM Handbook Volume 3: Alloy Phase Diagrams. 1992. p. 1741



**Percy Williams Bridgman (1882-1961,  
1946 Nobel Prize in Physics) –  
inventor of high pressure anvils technique**

## Mechanical alloying by high pressure torsion

- Severe plastic deformation (SPD) is used to produce ultrahigh-grained materials with a high proportion of high-angle boundaries. This leads to the achievement of promising characteristics of SPD-processed materials;
- High pressure torsion (HPT) is known for that it allows to achieve the greatest strains among all methods of severe plastic deformation;
- HPT is suitable to realize mechanical alloying and has some advantages contrary to ball milling



# Mechanical alloying by high pressure torsion

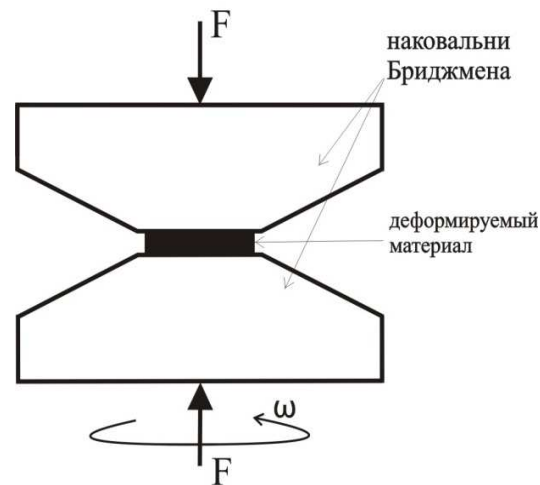


Fig. 1. The deformation scheme by the HPT method (a) and the image of the installation (b).  $F$  is the force produced by the hydraulic press;  $\omega$  - angular velocity of torsion of Bridgman anvil

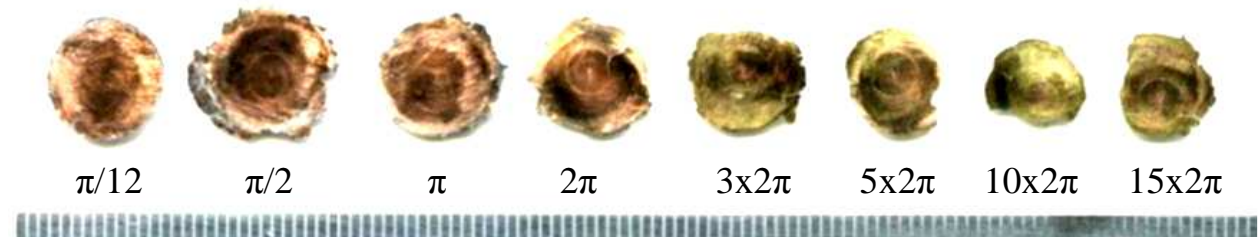


Fig. 2. Samples of the Cu-Zn system after the HPT treatment for various angles of rotation.

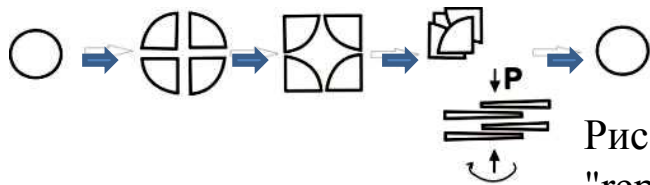


Рис. 3. Scheme of cutting and deformation of the sample during "reprocessing" or 3-stage "deformation" [1]

## Investigated components

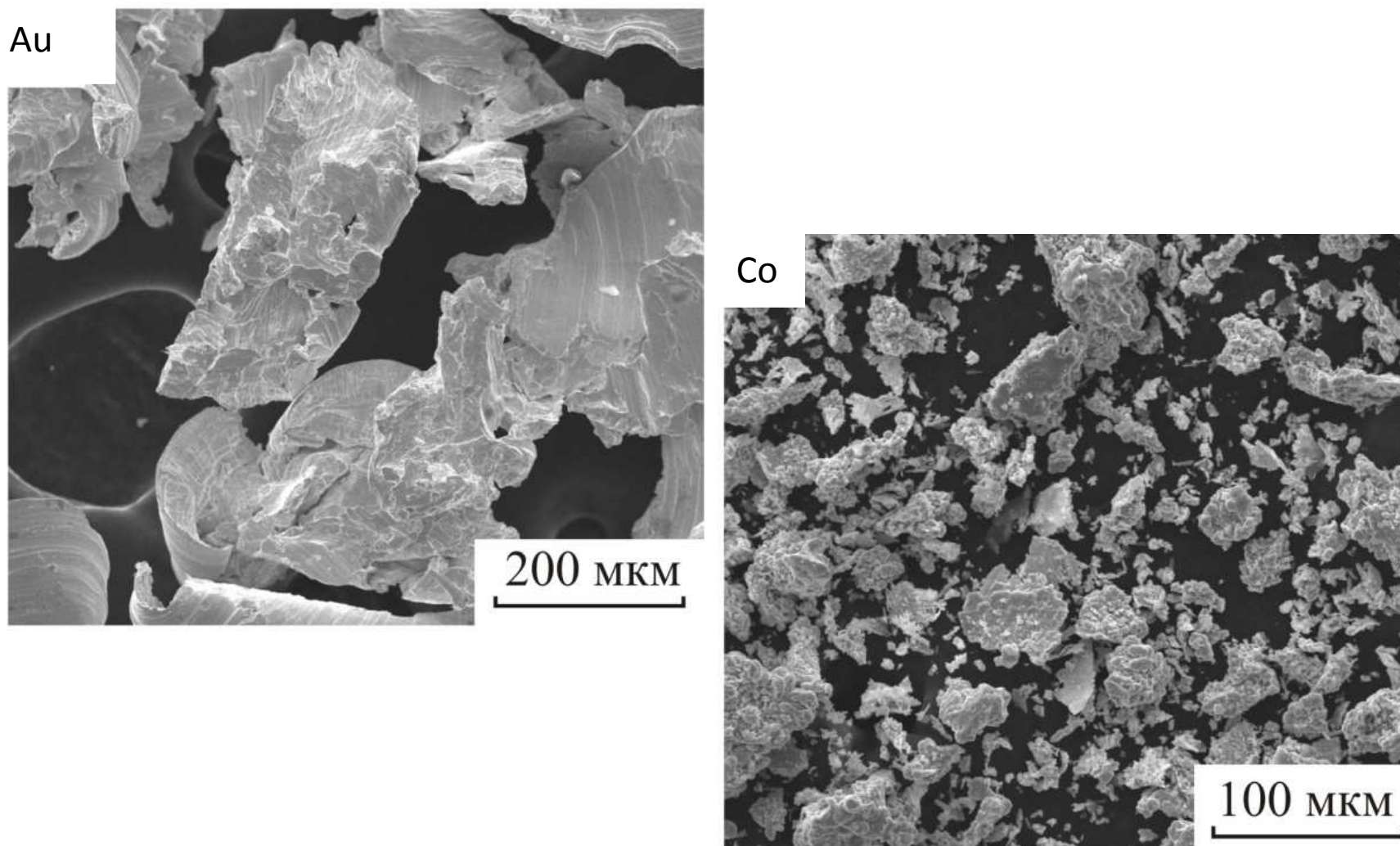
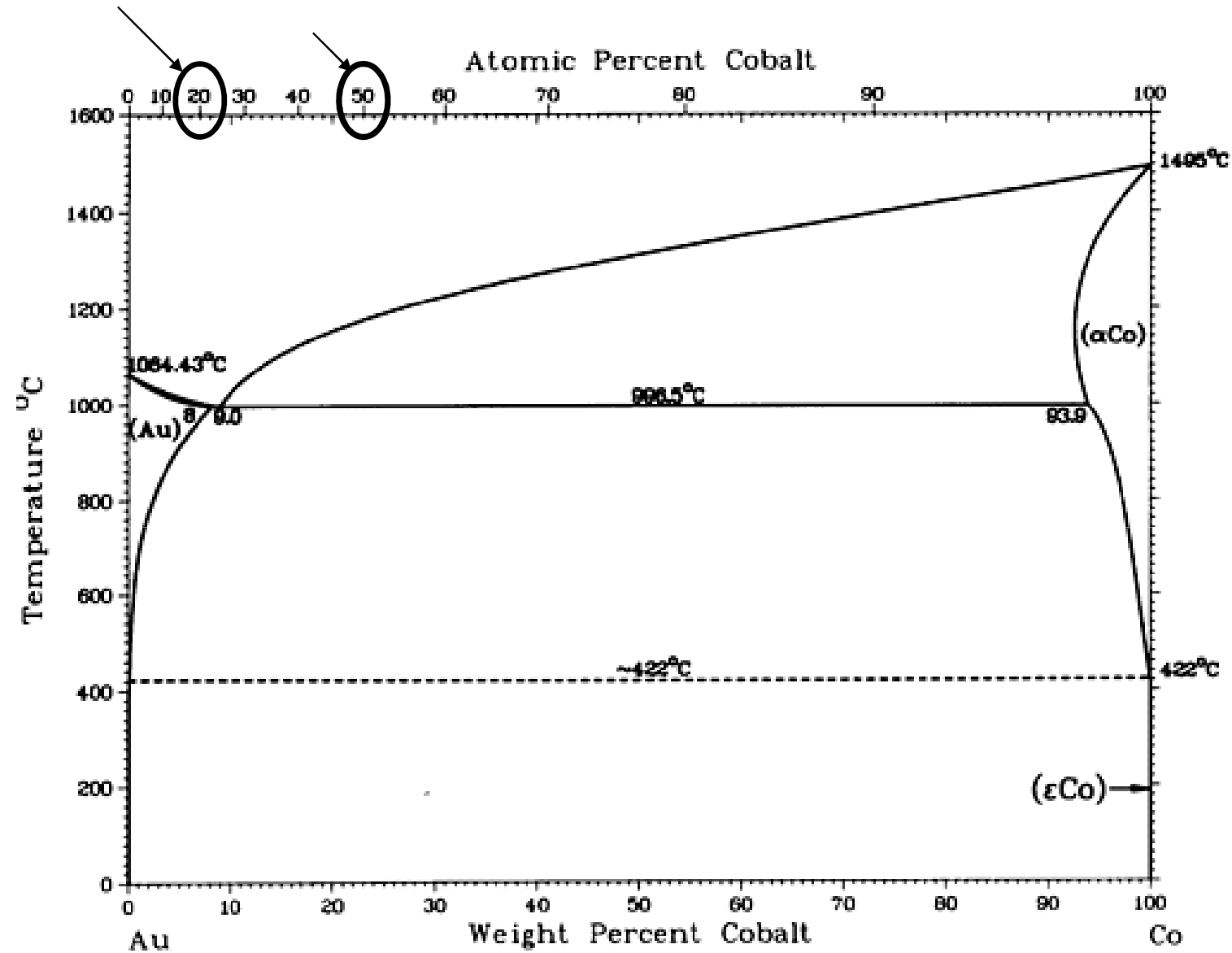


Fig. 3. The initial state of the powders. Scanning electron microscopy



ASM Handbook Volume 3: Alloy Phase Diagrams. 1992. p. 1741

# High-pressure torsion

- HPT was carried out at room temperature and at the temperature of liquid nitrogen. The homologous temperature  $T_{def}/T_m$  at 293 K was 0.22 for gold and 0.17 for cobalt; whereas at 80 K, it was 0.06 for gold and 0.05 for cobalt, which eliminated dynamic recrystallization.
- .. at pressure of 8 and 11 GPa in the Bridgman anvils with working areas 5 mm in diameter and made of tungsten carbide WC6 with a hardness of 92 HRC. The pressure was no less than 0.30 and no more than 0.41 of the shear modulus of gold, and not less than 0.11 and no more than 0.15 of that of cobalt, which is a sufficient value for their plastification under pressure.
- After deformation, the samples took the shape of a high-pressure cell in the form of a biconvex lens 100–120  $\mu\text{m}$  thick in the center and 40  $\mu\text{m}$  thick at the periphery.
- The angular velocity of deformation was the same for all processing modes and was 1 rev/min; the angle of anvil revolution was 1–40.
- To reduce the deformation-induced structure inhomogeneity along the radius, processing was performed in a three-stage mode (slide No. 5)



# Methods of research of HPT produced alloys

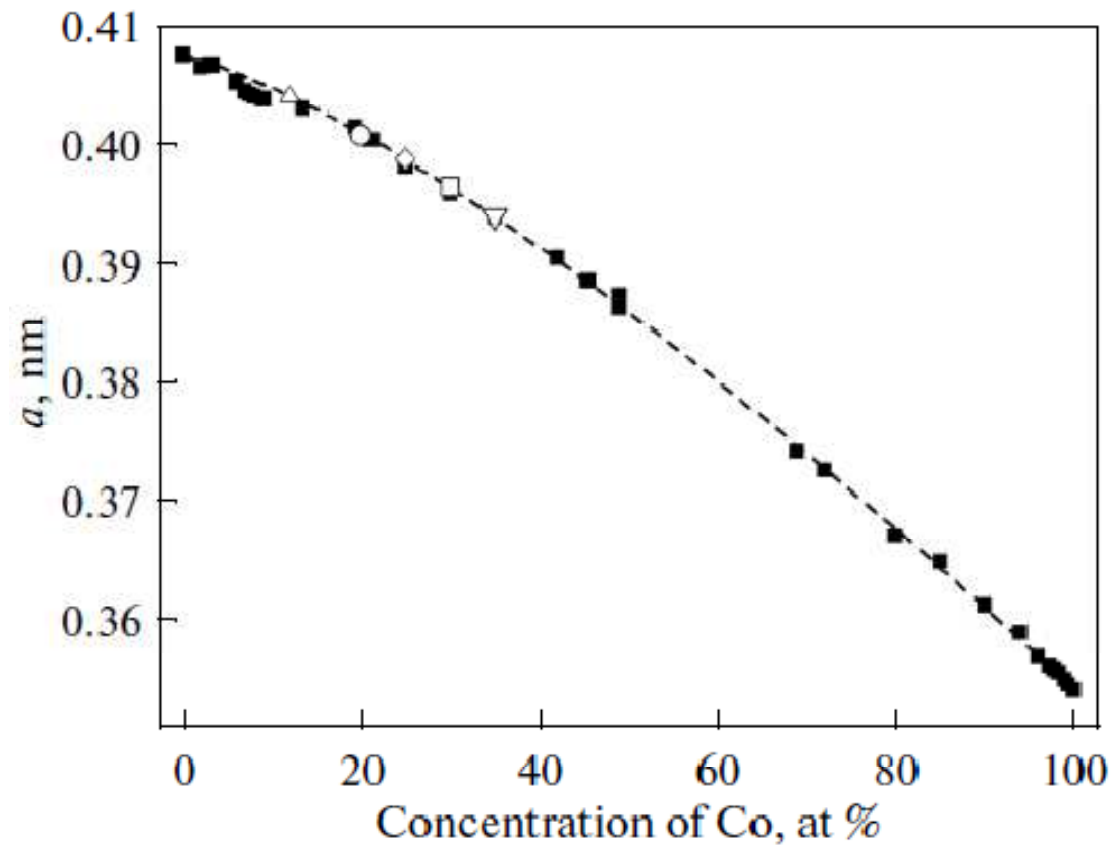
1. The structure of the samples was examined by X-ray diffraction (XRD) method in transmission synchrotron radiation (SR) in a beam with a cross section of  $0.3 \times 0.3 \text{ mm}^2$  at a wavelength of 0.03685 nm. A MAR-345 detector was used to record an SR diffraction pattern. SR diffraction patterns were transformed into traditional plots of the intensity–diffraction  $2\theta$ -angle dependences suitable for subsequent computational processing. The lattice parameter was calculated from the XRD peak positions, and, then, used to find the cobalt concentration in the gold-based solid solution. This method of transmission survey with a small-in-section beam allow us to evaluate the structural state of a sample over its entire thickness and certify the state with a precise estimation of the true strain.

The SR XRD performed on the 4th channel of the SR of the VEPP-3 accelerator in BINP SB RAS in Experimental station "Diffractometry in the "hard" X-ray range“ by A. Ancharov.

2. Fracture analysis by means of scanning electron microscopy with additional elemental analysis with the help of energy dispersive analyzer \* on SEM QUANTA-200 Pegasus \*. To do this, after the HPT, a diametric fracture of the disk specimens was made and the morphology of the surface and the character of the break on the SEM were studied;
3. Microhardness measurements with Microhardness Meter-3 (PMT-3);

\* Studies on SEM and TEM were carried out in the Department of Electron Microscopy of the Center for Testing the Center for Nanotechnologies and Advanced Materials, IMP UB RAS

Lattice parameter as a function of the cobalt content in the Au–Co system;  
(black squares) literature [1,2]



1. Zh. Xinming, H. R. Khan, and Ch. J. Raub, "Study of metallurgical and electrodeposited Au–Co metastable solid solutions," *J. LessCommon Met.* **96**, 249–256 (1984).
2. H. Okamoto, T. B. Massalski, T. Nishizawa, and M. Hasebe, "The Au–Co (Gold–Cobalt) system," *Bull. Alloy Phase Diagrams* **6**, 449–454 (1985).

# X-ray analysis of $\text{Au}_{80}\text{Co}_{20}$ at. % HPT-alloys

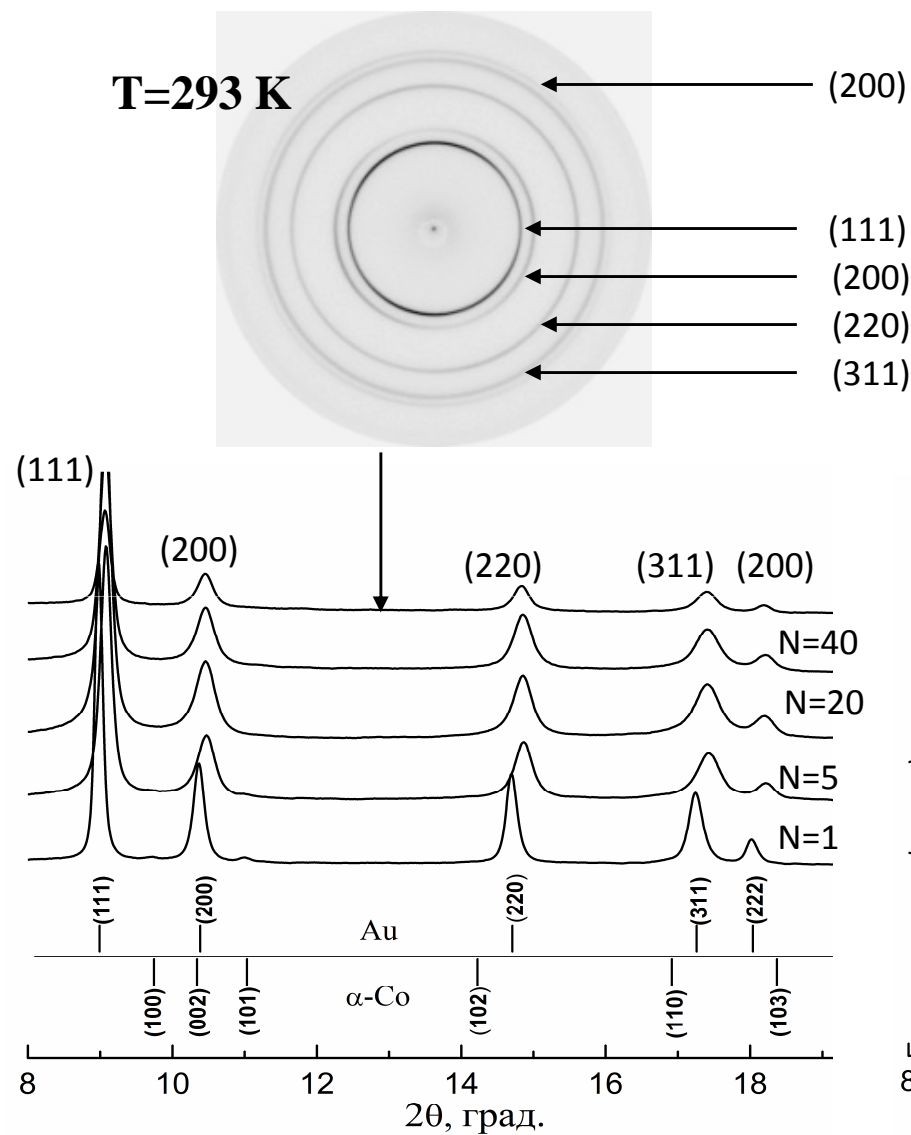


Fig. 1. XRD patterns in SR from alloys obtained by deformation for a different number of anvil revolutions at room temperature

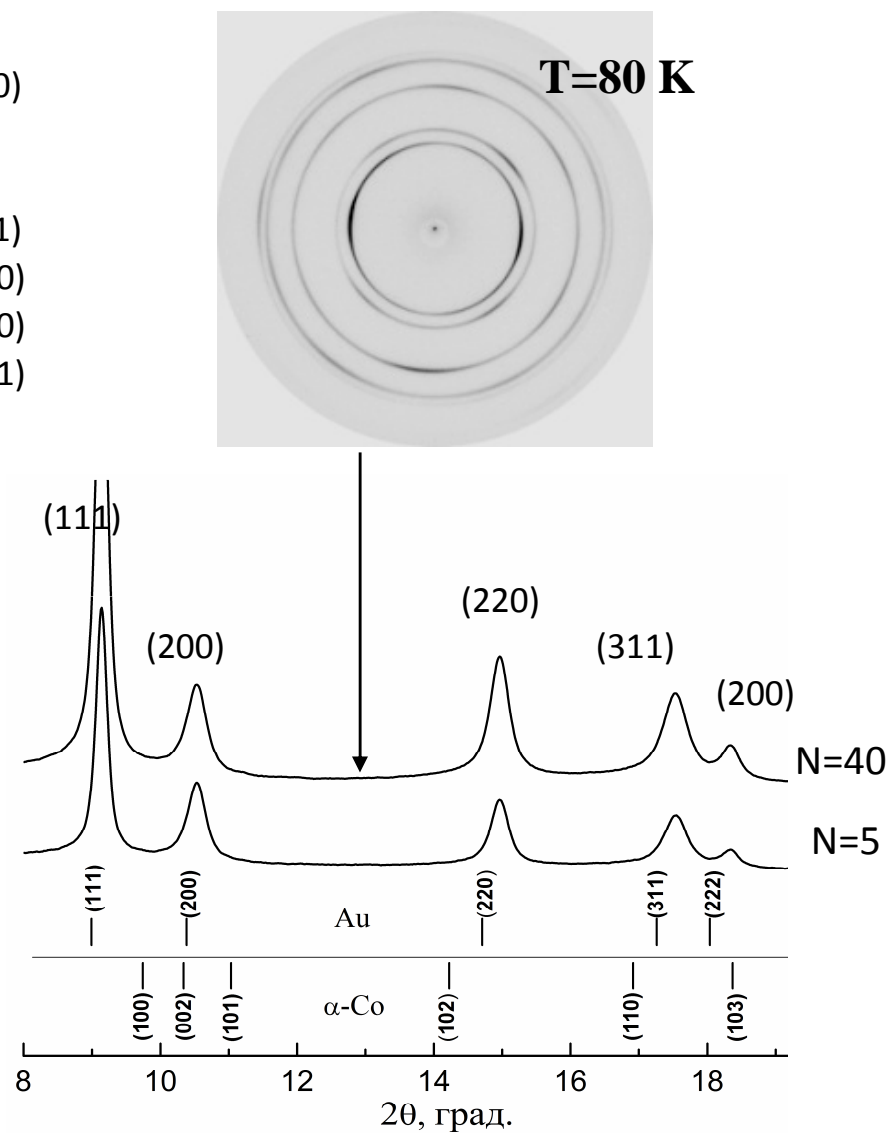


Fig. 2. XRD patterns in SR from alloys obtained by deformation for a different number of anvil revolutions at cryogenic temperature

# X-ray analysis of $\text{Au}_{80}\text{Co}_{20}$ at. % HPT-alloys

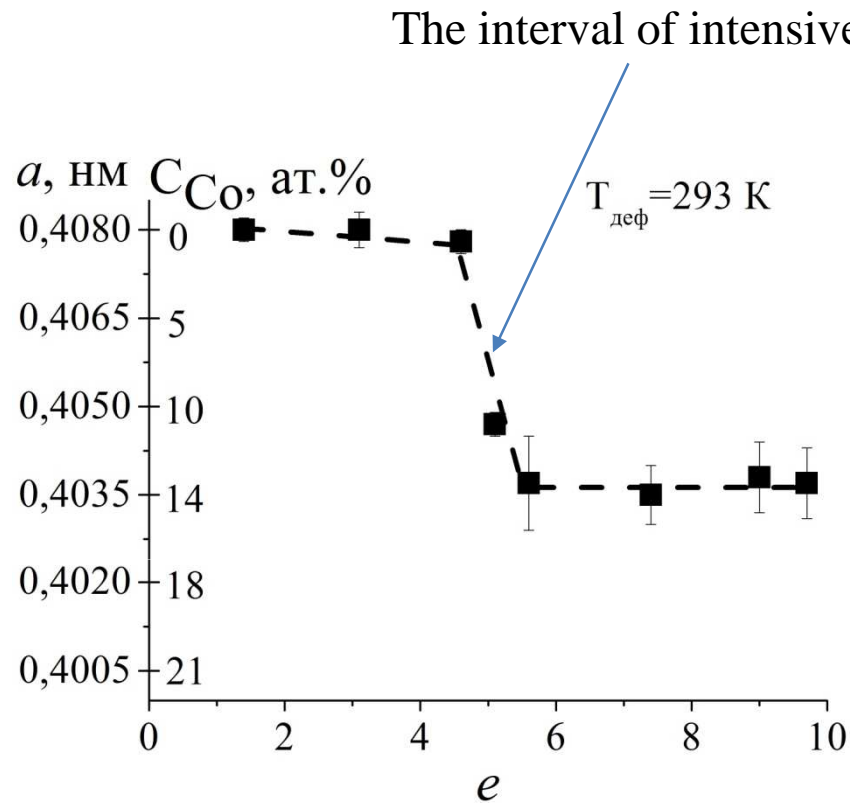


Fig. 1. Dependence of the values of the lattice parameter of solid solutions obtained at 293 K with increasing true deformation

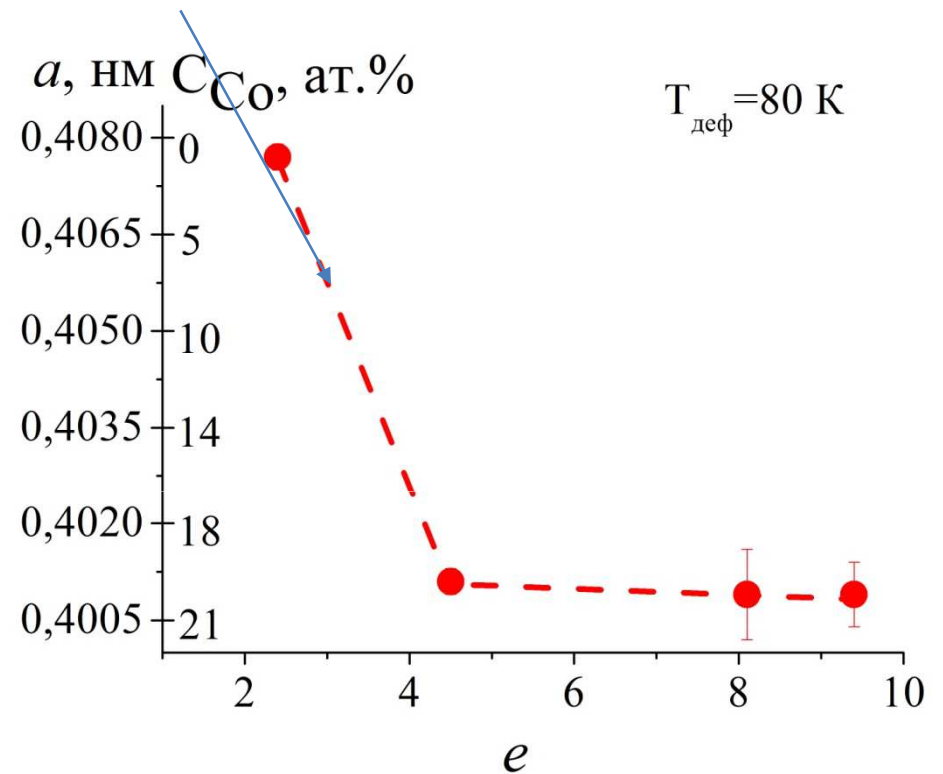


Fig. 2. Dependence of the values of the lattice parameter of solid solutions obtained at 80 K with increasing true deformation

# Hardness distribution along the radii of the $\text{Au}_{80}\text{Co}_{20}$ at. % HPT-samples

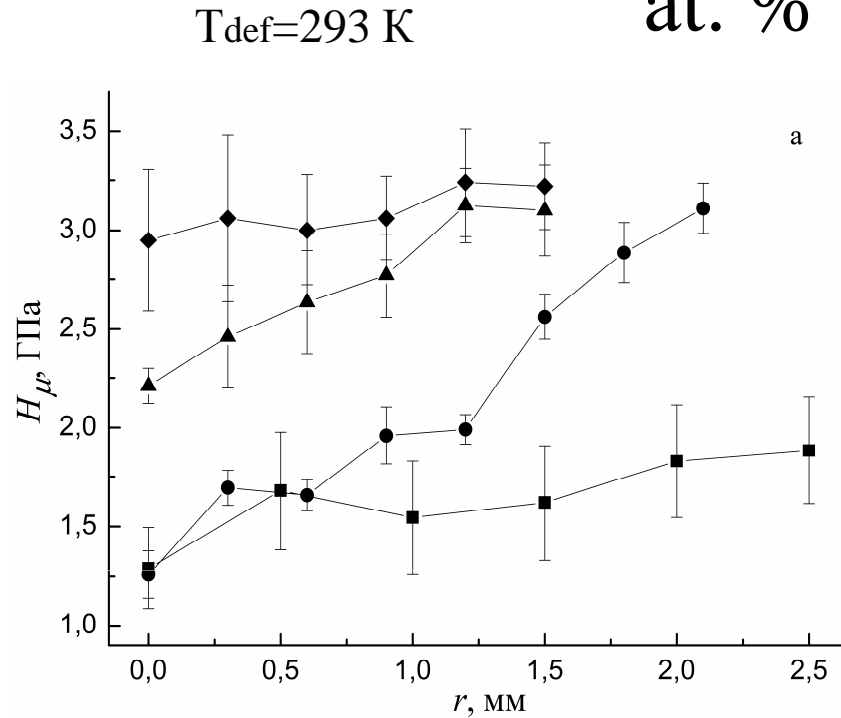


Fig. 3. Samples were obtained by rotating at room temperature to :

- – 1 turn;
- – 5 turns;
- ▲ – 20 turns;
- ◆ – 3-stage reprocessing (293 K)

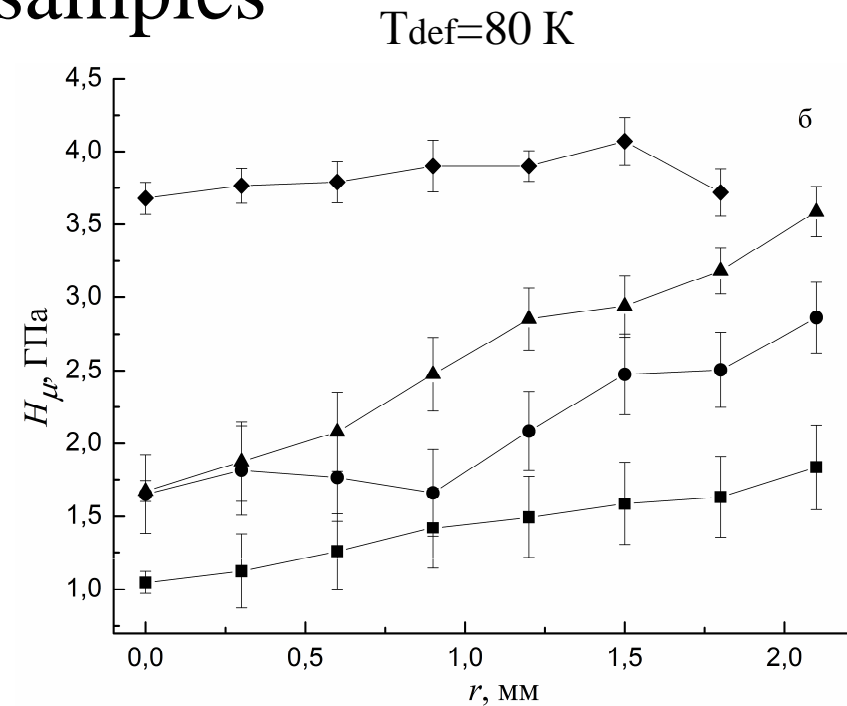


Fig. 4. Samples were obtained as a result of rotation at cryogenic temperature at :

- – 1 turn;
- – 5 turns;
- ▲ – 20 turns;
- ◆ – 40 turns(80 K)

# Dependence of hardness on the strain of $\text{Au}_{80}\text{Co}_{20}$ at. % HPT-samples

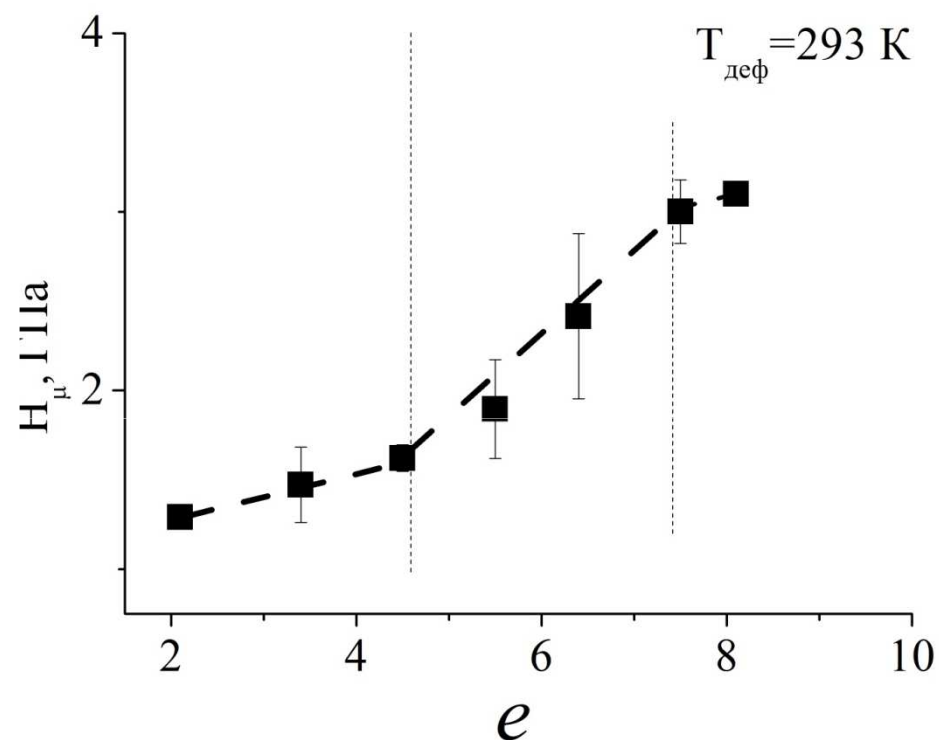


Fig. 5. Samples from the initial mixture  $\text{Au}_{80}\text{Co}_{20}$ , at. %, obtained by deformation at room temperature

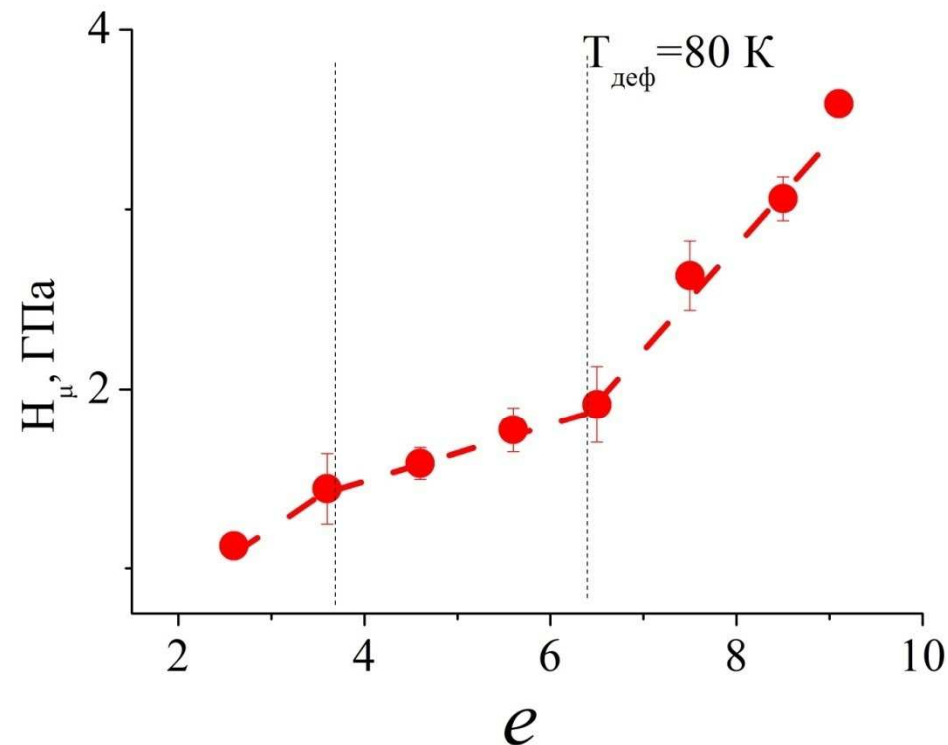


Fig. 6. Samples from the initial mixture  $\text{Au}_{80}\text{Co}_{20}$ , at. %, obtained by deformation at cryogenic temperature

# SEM fractographic analysis of Au<sub>50</sub>Co<sub>50</sub> at. % HPT-alloys

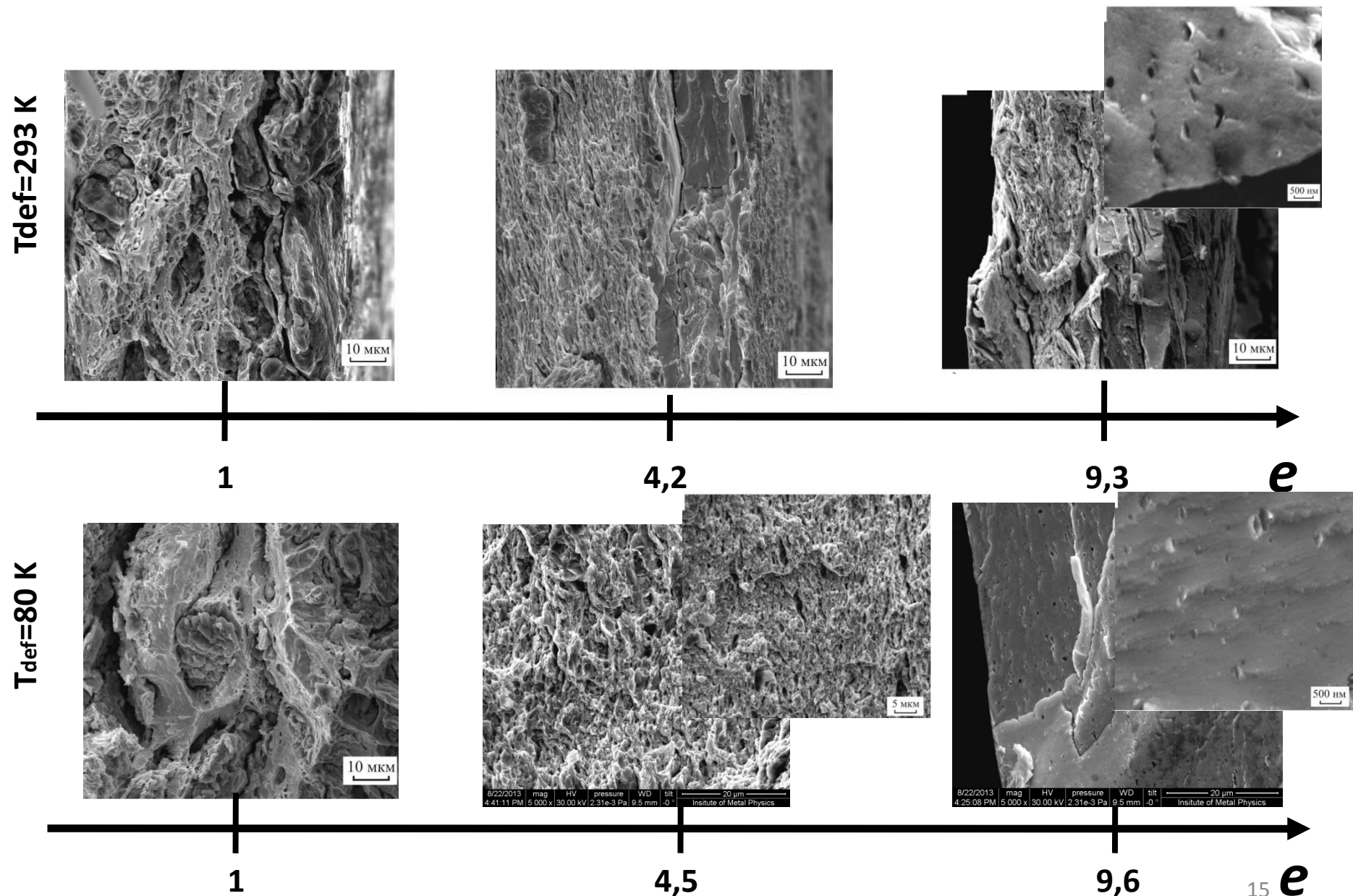


Fig. 7. Dependence of the morphology of the fracture surface of the samples on the strain value for the room and cryogenic temperature of the experiment



# Energy-dispersive analysis of $\text{Au}_{50}\text{Co}_{50}$ at. % HPT-alloys

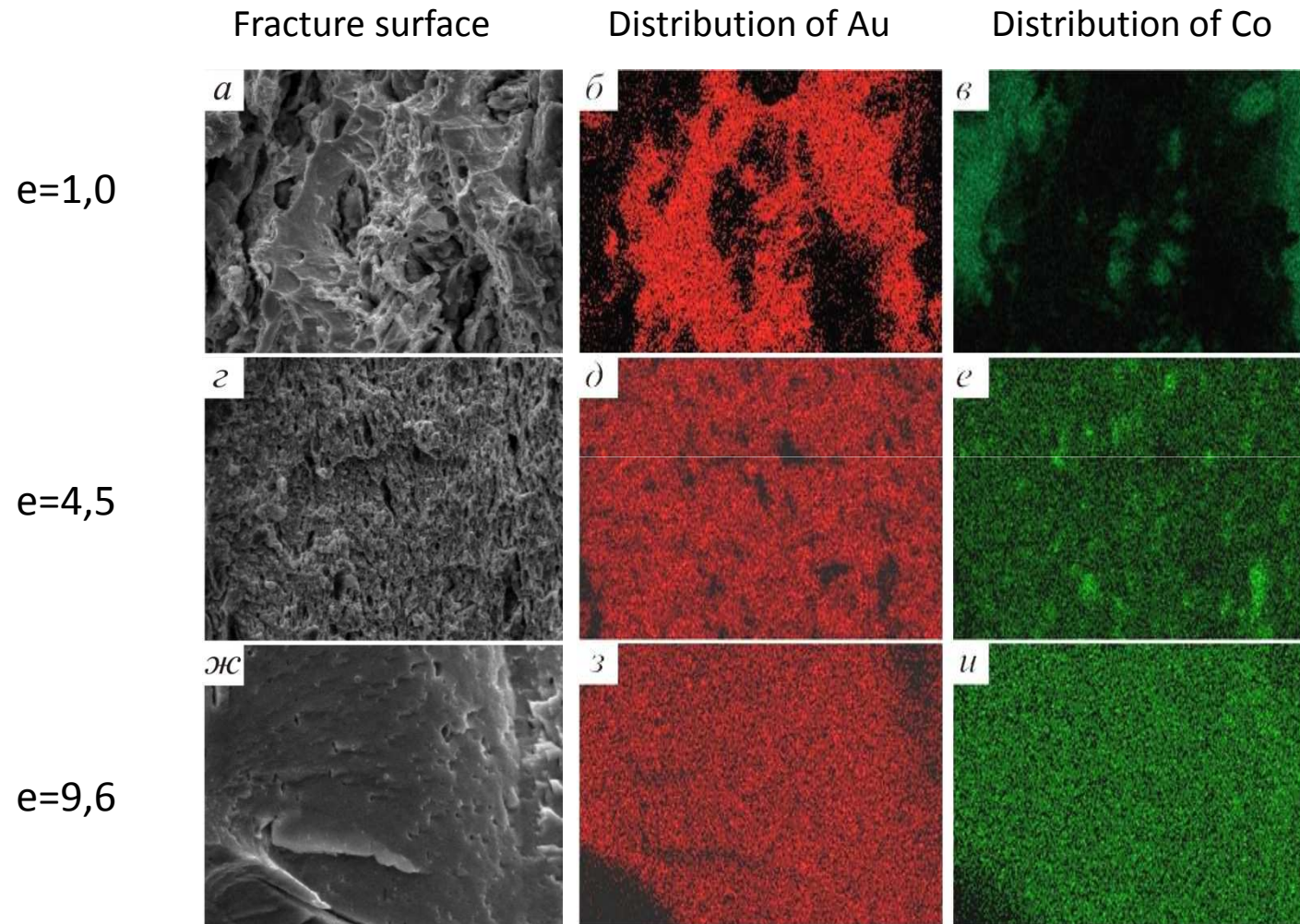


Fig. 8. Distributions of Au and Co on the surface of fractures of samples obtained by HPT at 80 K



# Conclusions

- Various methods have shown the presence of staging during mechanical alloying.
- (i) Particles of the components are slightly deformed, the contact between the components is small. As a result, the processes of mutual diffusion are difficult.
- (ii) Intensive process of mutual mixing at various levels as a result of increased deformation of the components and their mutual contact
- (iii) Saturation of the processes of deformation and dissolution
- The components of the studied system themselves determine the presence of decay processes, which are more difficult during cryodeformation.

# General on $\text{Au}_{80}\text{Co}_{20}$ & $\text{Au}_{50}\text{Co}_{50}$ at. % HPT-alloys

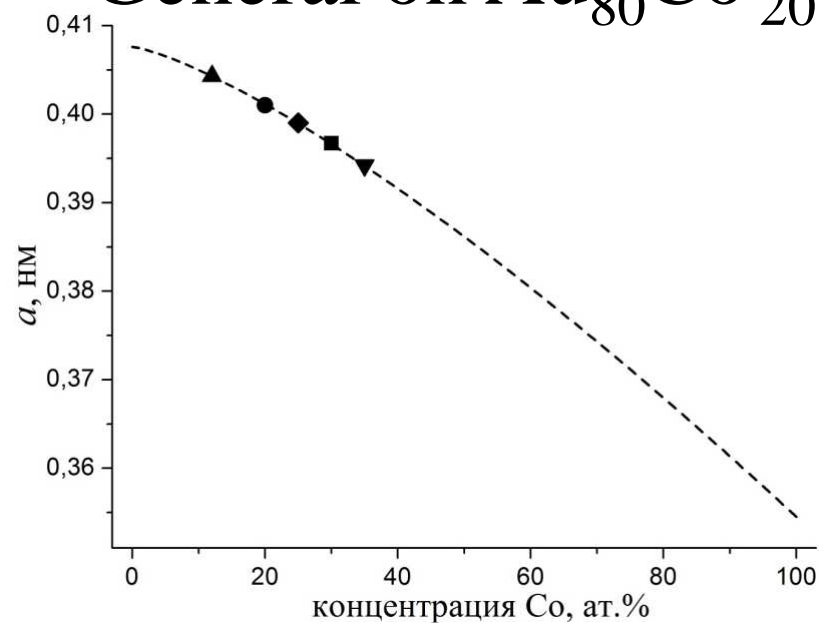


Fig. Dependence of the lattice period of the Au-Co system on the cobalt concentration.

----- [1,2]

Composition of charge	Au80Co20	Au80Co20	Au50Co50	Au50Co50	Au50Co50
Давление обработки	11 GPa	11 GPa	8 GPa	8 GPa	11 GPa
Processing pressure	293 K	80 K	293 K	80 K	80 K
Treatment mode (deformation)	N=40, 3x10	3x10	3x10	3x10	N=40
The Co content in the solid solution (lattice parameter)	12,1 at.% (0,4043 nm)	20,0 at.% (0,4010 nm)	24,6 at.% (0,3990 nm)	30,0 at.% (0,3967 nm)	35,0 at.% (0,3942 nm)

[1] H. Okamoto, T. B. Massalski, T. Nishizawa, M. Hasebe. The Au-Co (Gold-Cobalt) system. Bulletin of Alloy Phase Diagrams. 1985. Volume 6, Issue 5, pp 449-454

[2] Zhou Xinming, H. R. Khan and Ch. J. Raub. Study of metallurgical and electrodeposited Au-Co metastable solid solutions. Journal of the Less-Common Metals, 96 (1984) pp. 249-256

# Thank you for attention!

The research was carried out within the state assignment of Ministry of Science and Higher Education of the Russian Federation (theme “Pressure” No. AAAA-A18-118020190104-3),  
supported in part by RFBR (project No. 19-32-60039).